[5]This transition is erroneously listed as 965.8 keV in Table I of Ref. 4.
[6]R. L. Hershberger, K. E. G. Löbner, R. Lutter, D. Proetel, and F. Riess, Universität München Annual Report, 1975, p. 78.
[7]L. Richter, H. Backe, E. Kankeleit, F. Weik, and R. Willwater, Phys. Lett. 71B, 74 (1977).
[8]F. W. N. De Boer, L. K. Peker, P. Koldewijn, and J. Konijn, Z. Phys. A 284, 267 (1978).
[9]S. G. Nilsson, C. F. Tsang, A. Soviczewski, Z. Szymanski, S. Wycech, C. Gustafson, I. L. Lamm, P. Möller, and B. Nilsson, Nucl. Phys. A131, 1 (1969).
[10]R. Bengtsson, I. Hamamoto, and B. Mottelson, Phys. Lett. 73B, 259 (1978).
[11]A. Faessler and M. Ploszajczak, Phys. Lett. 76B, 1 (1978).

Spontaneous Singularity in Three-Dimensional, Inviscid, Incompressible Flow

Rudolf H. Morf[(a)]
Lyman Laboratory of Physics, Harvard University, Cambridge, Massachusetts 02138

and

Steven A. Orszag
Department of Mathematics, Massachusetts Institute of Technology, Cambridge, Massachusetts 02139

and

Uriel Frisch
Observatoire de Nice, Centre National de la Recherche Scientifique, F-06300 Nice, France
(Received 10 December 1979)

The results obtained by series-analysis techniques applied to the time evolution of the inviscid Taylor-Green vortex support the conjecture that vortex lines may be stretched an infinite amount in a finite time.

The classical theorems[1] of Kelvin and Helmholtz imply that, in an inviscid incompressible fluid of constant density, vortex lines move with the fluid and vorticity is amplified proportional to the stretching of a vortex line element. These theorems are central to the understanding of the dynamics of high-Reynolds-number flows.

For boundary-free flow, the Kelvin and Helmholtz theorems imply that an initially smooth, inviscid flow remains smooth so long as vortex lines are stretched only a finite amount. Indeed, the restriction of the flow to two space dimensions precludes vortex-line stretching so global regularity follows.[2] However, in three dimensions, vortex lines can twist, tangle, turn, and stretch. It is conceivable that flow velocities remain bounded and, still, a singularity of the flow appears spontaneously after a finite time in the interior of the flow.[3] Segments of vortex lines could develop infinite length by becoming intricately wound up and twisted without the end points of the segment being separated by an infinite distance. These properties of inviscid flow have been the subject of some speculation in the past.[4-6] In this Letter we offer evidence of the correctness of the conjecture that spontaneous singularities occur in three-dimensional inviscid incompressible flows. While the results to be presented below are clearly not a rigorous proof of singularity, they provide the first quantitative data that support the existence of the putative singularity.

Our results are obtained by solving the three-dimensional Euler equations as power series in time t with the simple initial conditions introduced by Taylor and Green.[7] The resulting power-series expansions are analyzed using techniques developed for the study of singularities in critical phenomena.[8] The flow is the solution of the incompressible Euler equations which are, in Fourier representation,[4]

$$\frac{\partial u_\alpha(\vec{k};t)}{\partial t} = -i\sum_{\beta,\gamma=1}^{3} k_\beta\left(\delta_{\alpha\gamma}-\frac{k_\alpha k_\gamma}{k^2}\right) \times\sum_{\vec{p}} u_\beta(\vec{p};t)\,u_\gamma(\vec{k}-\vec{p};t). \quad (1)$$

The initial conditions in real space are[5,7,9]

$$v_1(x_1,x_2,x_3;t=0)=\cos x_1\sin x_2\cos x_3, \quad (2)$$

$$v_2(x_1,x_2,x_3;t=0)=v_1(x_2,-x_1,x_3;t=0), \quad (3)$$

$$v_3(x_1,x_2,x_3;t=0)=0. \quad (4)$$

Our approach is to examine the structure of global flow properties for singular behavior. The generalized enstrophy and its power series in t are defined, for integer p, by[10]

$$\Omega_p(t) \equiv \sum_{\vec{k}} k^{2p} |\vec{u}(k, t)|^2 = \sum_{n=0}^{\infty} A_n^{(p)} t^{2n}. \qquad (5)$$

Notice that $\Omega_0(t)$ is twice the kinetic energy while $\Omega_1(t)$ is the enstrophy (half the mean square vorticity). For smooth inviscid flows, $\Omega_0(t)$ is constant, so singularities can only show up in the power series for Ω_p with $p>0$.

Taylor and Green[7] calculated analytically the power-series coefficients of the solution to (1)–(4) to order t^3 and the coefficients of Ω_1 to order t^4. Van Dyke[11] computed Ω_1 to order t^8 numerically. These low-order expansions give no hint of a possible physical singularity. In order to explore the analytic structure of the flow, it is necessary to go far beyond.

We have calculated Ω_p to order t^{44} for $p \leqslant 4$. The expansion coefficients $A_n^{(p)}$ for the solution of (1)–(4) are obtained by calculating time derivatives $\partial^m \vec{u}(\vec{k}; t=0)/\partial t^m$ with use of (1) recursively. With the initial conditions (2)–(4), the first nonzero time derivative of $\vec{u}(\vec{k}; 0)$ is of order $m \geqslant \max_\alpha ||k_\alpha| - 1|$. Therefore, computation of $A_n^{(p)}$ from (5) requires that time derivatives of $\vec{u}(\vec{k}; 0)$ be known up to order $2n - \max_\alpha ||k_\alpha|-1|$.

The nonlinear term in (1) is computed by direct summation[12] with 29-digit precision. An analysis[13] of the effect of roundoff error indicates that each computed coefficient $A_n^{(p)}$ has at least ten significant digits. In Table I, we list $A_n^{(p)}$ $(0 \leqslant n \leqslant 22,$ $1 \leqslant p \leqslant 4)$ to five places.

We first perform an analysis of the series for Ω_1 as a function of t^2 using Padé approximants. In Table II, we list the location t^2 of the smallest positive real pole of the $[N/N]$ and $[N/N+1]$ Padé approximants to Ω_1. These results suggest real singularities for $t = \pm t_*$, $t_* \simeq 5.2$.

Padé approximants to $d \ln\Omega_1/dt^2$ reveal a complicated analytical structure. First, they show that the radius of convergence of the series for Ω_1 is determined by a singularity at $t^2 \simeq -5$. Indeed, inspection of Table I shows that $A_n^{(1)}/A_{n+1}^{(1)}$ is close to -5 for large n. Second, these Padé approximants indicate other singularities at t_*^2 and near $t^2 \simeq -5.9 \pm i3.5$, $t^2 \simeq 1.0 \pm i6.7$, and $t^2 \simeq -9$. In order to focus on the apparent physical singularity at t_*^2, we perform the Euler transformation

$$w = 6t^2/(t^2+5) \qquad (6)$$

and analyze the resulting series

$$\Omega_p(t) \equiv \bar{\Omega}_p(w) = \sum_{n=0}^{\infty} B_n^{(p)} w^n. \qquad (7)$$

The radius of convergence of the series (7) for $\bar{\Omega}_p(w)$ is determined by the image of the physical singularity at t_*^2. In Fig. 1, we plot the ratios $r_n^{(p)} = B_n^{(p)}/B_{n-1}^{(p)}$ for $1 \leqslant p \leqslant 4$ as a function of $1/n$.

For $p = 2, 3, 4$ these ratios decrease monotonically with increasing n and the extrapolation to $n = \infty$ is consistent with a common intersection at $1/w(t_*) = r_\infty \simeq 0.197$ or $t_* \simeq 5.2$. The ratios $r_n^{(1)}$ appear to be affected by singularities outside the radius of convergence and the extrapolation to $n = \infty$ is less well defined, although consistent with

TABLE I. Coeffeicients $A_n^{(p)}$ of the series expansion (5) of $\Omega_p(t)$ in powers of t^2.

N	$A_N^{(1)}$	$A_N^{(2)}$	$A_N^{(3)}$	$A_N^{(4)}$
0	7.50000×10^{-1}	2.25000×10^{0}	6.75000×10^{0}	2.02500×10^{1}
1	7.81250×10^{-2}	8.59375×10^{-1}	7.57812×10^{0}	6.27344×10^{1}
2	5.91856×10^{-3}	1.83535×10^{-1}	3.86707×10^{0}	7.30880×10^{1}
3	-2.78436×10^{-4}	1.78070×10^{-2}	1.09499×10^{0}	4.21618×10^{1}
4	6.10482×10^{-5}	3.54517×10^{-3}	2.90691×10^{-1}	1.78215×10^{1}
5	-9.63613×10^{-6}	1.00989×10^{-4}	6.27515×10^{-2}	6.88633×10^{0}
6	1.23765×10^{-6}	3.88235×10^{-5}	1.51507×10^{-2}	2.66539×10^{0}
7	-1.30017×10^{-7}	2.23680×10^{-6}	3.01585×10^{-3}	9.07388×10^{-1}
8	1.15077×10^{-8}	-7.27553×10^{-7}	4.45824×10^{-4}	2.65742×10^{-1}
9	-4.06899×10^{-10}	3.00295×10^{-7}	9.56613×10^{-5}	7.25449×10^{-2}
10	-1.57226×10^{-10}	-8.30095×10^{-8}	3.40805×10^{-6}	1.62495×10^{-2}
11	5.64571×10^{-11}	2.02138×10^{-8}	2.73360×10^{-6}	3.64934×10^{-3}
12	-1.36969×10^{-11}	-4.59369×10^{-9}	-3.20748×10^{-7}	6.17595×10^{-4}
13	2.99202×10^{-12}	1.00820×10^{-9}	1.05275×10^{-7}	1.18878×10^{-4}
14	-6.19920×10^{-13}	-2.14055×10^{-10}	-2.14857×10^{-8}	1.37210×10^{-5}
15	1.24509×10^{-13}	4.43761×10^{-11}	4.80541×10^{-9}	2.62510×10^{-6}
16	-2.47745×10^{-14}	-9.08095×10^{-12}	-9.90282×10^{-10}	1.24648×10^{-7}
17	4.92528×10^{-15}	1.83786×10^{-12}	2.02179×10^{-10}	4.79322×10^{-8}
18	-9.77190×10^{-16}	-3.68247×10^{-13}	-3.98009×10^{-11}	-2.23338×10^{-9}
19	1.93754×10^{-16}	7.33436×10^{-14}	7.60907×10^{-12}	9.96301×10^{-10}
20	-3.85060×10^{-17}	-1.45521×10^{-14}	-1.41005×10^{-12}	-1.02271×10^{-10}
21	7.67013×10^{-18}	2.87657×10^{-15}	2.51732×10^{-13}	1.56825×10^{-11}
22	-1.53011×10^{-18}	-5.67226×10^{-16}	-4.28522×10^{-14}	1.06314×10^{-13}

TABLE II. Locations t^2 of the smallest positive real pole of the $[N/N]$ and $[N/N+1]$ Padé approximations to $\Omega_1(t)$ as a function of t^2.

N	$[N/N]$	$[N/N+1]$
7	33.72	27.33
8	26.53	27.58
9	26.99	27.23
10	26.99	27.51

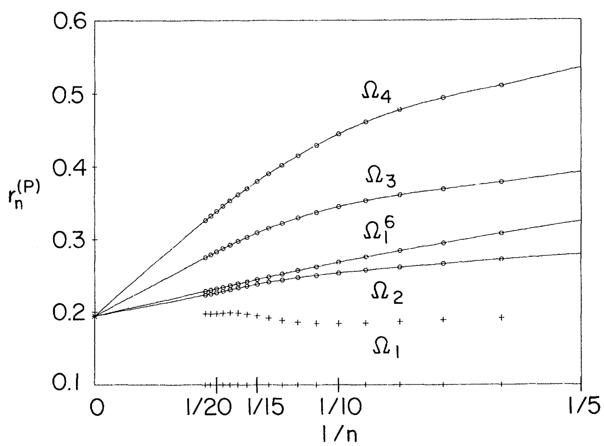

FIG. 1. A plot of the ratios $r_n^{(p)}$ defined in Eq. (8) vs $1/n$. The solid curves are piecewise quadratic polynomial fits to the discrete data.

a value $r_\infty \simeq 0.197$. Analyzing instead the expansion of $[\Omega_1(t)]^k$, $k = 2, 3, 4, \ldots$, in powers of w leads to ratios which can be extrapolated with confidence. The ratios for $k = 6$ are also plotted in Fig. 1. The extrapolation is insensitive to the value of k and consistent with a common intersection at r_∞. The deviation from linearity is minimized for $k \simeq 5$, for which the data almost exactly coincide with $r_n^{(2)}$ for large n. Lacking analytical information about the asymptotic behavior of $r_n^{(p)}$ as $n \to \infty$, we refrain from quoting an error estimate for r_∞ or t_*.

All these results suggest that the asymptotic behavior of $r_n^{(p)}$ is of the form

$$r_n^{(p)} \sim r_\infty[1 + (\gamma_p - 1)/n + \ldots] \quad (n \to \infty), \tag{8}$$

implying power-law behavior of Ω_p near t_* of the form $(t_* - t)^{-\gamma_p}$ with critical exponents

$$\gamma_1 \simeq 0.8 \pm 0.1, \quad \gamma_2 \simeq 4.2 \pm 0.3, \quad \gamma_3 \simeq 9.9 \pm 0.5, \quad \gamma_4 \simeq 16 \pm 1. \tag{9}$$

The value of γ_1 is obtained by analyzing the series for Ω_1^k; the result is insensitive to the power $k \gtrsim 3$ used for the analysis.[14]

At this point, we again raise the question of numerical precision. With the assumption that the critical exponent γ_1 at t_* is roughly 0.8, the contribution to the coefficient $A_{22}^{(1)}$ from this singularity is then about 10^{-32} times smaller than its contribution to $A_0^{(1)}$. For $\gamma_2 \simeq 4.2$, $\gamma_3 \simeq 9.9$, and $\gamma_4 \simeq 16$, the corresponding factors are about 10^{-28}, 10^{-23}, and 10^{-19}, respectively. Since our calculations are accurate to about 10^{-27}, we infer that the calculations become unreliable for Ω_1 at order t^{36}, for Ω_2 at order t^{40}, while the calculations for Ω_3 and Ω_4 are significant throughout. The series for $[\Omega_1(t)]^k$ ($k \gtrsim 5$) is also significant throughout.

At finite Reynolds numbers R, $\Omega_p(t)$ should remain finite for all $t > 0$. Direct numerical calculations[5] suggest nearly singular behavior at large R for $t \simeq 6$ with $\Omega_1(t)/R$ finite as $R \to \infty$ for $t \gtrsim 6$. In fact, the real singularity at t_* when $R = \infty$ should split into complex-conjugate singularities for finite R.[15]

Since the Taylor-Green vortex is a prototype for vortex stretching, we expect that singularities similar to that discussed here should develop spontaneously in general three-dimensional inviscid flows. The structure of the flow near breakdown has important consequences for small-scale turbulent flow structures and their intermittency.[16] The present techniques may be useful in this analysis. It may also be productive to consider the flow near the singularity at t_* as the first manifestation of turbulence, with excitation at arbitrarily small spatial scales.[4-6, 17]

The present techniques may extend directly to the study of the analytic structure of inviscid magnetohydrodynamics[18] and stratified and free-surface flow problems.[19]

We should like to acknowledge helpful discussions with B. I. Halperin, H. P. Kraft, R. Petschek, and J. Thierry-Mieg. The computations were performed at the Computing Facility of the National Center for Atmospheric Research, Boulder, Colorado, which is supported by the National Science Foundation.

This work was supported in part by the Swiss National Science Foundation under Grant No. 82. 528.0.77, in part by the National Science Foundation under Grants No. DMR-77-10-10120 and No. ATM-7817092, and in part by the U. S. Office of Naval Research under Contract No. N00014-77-C-138.

[a] Present address: Laboratories R. C. A. Ltd., CH-8048 Zurich, Switzerland.

[1] G. K. Batchelor, *An Introduction to Fluid Dynamics* (Cambridge Univ. Press, Cambridge, 1967).

[2] W. Wolibner, Math. Z. 37, 698 (1933).

[3] It is known that the three-dimensional Euler equations have smooth solutions for a finite time, dependent on initial conditions. See, e.g., L. Lichtenstein, Math. Z. 23, 89 (1925) or D. G. Ebin and J. E. Marsden, Ann. Math. 92, 102 (1970).

[4] S. A. Orszag, in *Fluid Dynamics*, edited by R. Bali-

an and J. L. Peube (Gordon and Breach, London, 1977), p. 235.

[5]S. A. Orszag, in *Computing Methods in Applied Sciences and Engineering*, edited by R. Glowinski and J. L. Lions (Springer, Berlin, 1974), Pt. 2, p. 50.

[6]A. Brissaud, U. Frisch, J. Leorat, M. Lesieur, A. Mazure, A. Pouquet, R. Sadourny, and P. L. Sulem, Ann. Geophys. 29, 539 (1973).

[7]G. I. Taylor and A. E. Green, Proc. Roy. Soc. London, Ser. A 158, 499 (1937).

[8]D. S. Gaunt and A. J. Guttmann, in *Phase Transitions and Critical Phenomena*, edited by C. Domb and M. S. Green (Academic, London, 1974), Vol. 3, p. 181. Also, G. S. Rushbrooke, G. A. Baker, Jr., and P. J. Wood, *ibid.*, p. 246.

[9]These initial conditions are analytic in $\vec{x}$, so the flow remains so for at least a finite time. See C. Bardos, C. R. Acad. Sci. (Paris) 283A, 255 (1976).

[10]With the initial conditions (2)–(4), the fact that the series for $\Omega_p(t)$ involves only even powers of t follows from invariance under time reversal.

[11]M. D. Van Dyke, SIAM J. Appl. Math. 28, 720 (1975). Also, R. J. Fateman and S. A. Orszag (unpublished) used the algebraic manipulation program MACSYMA to compute $\Omega_1(t)$ to order t^{10} analytically.

[12]Even utilizing all the many symmetries (see Ref. 5) of the flow, the computation of Ω_p to order t^{44} with 29-digit precision required about 7 h on a CDC 7600 computer. Since the required work to calculate to order t^n scales as n^8, further computations are very costly. An alternative computational procedure is to use transform methods (see Ref. 5) to evaluate the nonlinear term in (1), which requires order $n^5 \ln n$ operations. Nevertheless, the code based on the present method is more efficient through order t^{50} because not all modes are excited at once.

[13]The error estimate is inferred from a comparison of the present double-precision results with single-precision calculations to order t^{28}. At order t^{28}, absolute errors in the single-precision results are about 10^{-14}, so that single-precision results lose all significance beyond order t^{30}. On this basis, we assume that the absolute errors in the double-precision results at order t^{44} are about 10^{-27}.

[14]Padé approximations to $d\ln\tilde{\Omega}_1/dw$ also show a real singularity at $t_* \simeq 5.2$ with a residue $-\gamma_1 \simeq -0.8$.

[15]U. Frisch and R. H. Morf, unpublished. They analyze the solutions to a nonlinear Langevin equation in time t with band-limited forcing and find that small-scale structure is intimately related to the distribution of singularities in the complex t plane.

[16]The critical exponents γ_p do not appear to lie in arithmetic progression. Thus, it seems that more than one significant length scale is responsible for flow breakdown near t_*.

[17]More recent studies of Ω_p with noninteger p (done with D. Meiron) suggest the preliminary result that a singularity appears at t_* for $p \gtrsim 0.3$. Further work is now underway to substantiate this result and its possible connection with the inertial-range turbulence spectrum. We remark that Ω_p is singular for $p \geq 1/3$ if the Kolmogorov $k^{-5/3}$ spectrum is established.

[18]S. A. Orszag and C. M. Tang, J. Fluid Mech. 90, 129 (1979).

[19]D. W. Moore, Proc. Roy. Soc. London, Ser. A 365, 105 (1979).

Nonlinear Inverse Bremsstrahlung and Heated-Electron Distributions

A. Bruce Langdon
Lawrence Livermore Laboratory, University of California, Livermore, California 94550
(Received 25 May 1979)

When $Zv_0^2/v_e^2 \gtrsim 1$, inverse bremsstrahlung results in a non-Maxwellian velocity distribution for which the absorption is reduced by up to a factor of 2 compared with the Maxwellian distribution usually assumed. Transport and atomic processes are also altered. Especially in materials with $Z \gg 1$, this is significant at lower intensities than for the well-known nonlinearity for which the measure is v_0^2/v_e^2.

Light absorption by inverse bremsstrahlung remains attractive in laser-induced fusion schemes, as compared with absorption by collective processes which heat a minority of the electrons to superthermal energies. These electrons preheat the target core and do not effectively drive an ablative implosion. To make inverse bremsstrahlung competetive it may require that the ion charge state Z greatly exceed 1. Especially in this case, but also for $Z=1$, I will demonstrate nonlinear modifications which take effect at lower intensities than the absorption nonlinearity analyzed many times before.[1-4] A second refinement removes the usual restriction that the light frequency must greatly exceed the collision frequency.

We reexamine the collisional absorption (inverse bremsstrahlung) of intense laser light in a dense plasma, considering heating and diffusion of electrons of various energies, the evolu-

